InAlN/GaN HEMT technology for robust HF receivers: An overview of the HF and LF noise performances

Séraphin Dieudonné Nsele, Jean-Guy Tartarin, Laurent Escotte, S Piotrowicz, S Delage

InAlN/GaN HEMT Technology for Robust HF Receivers: an Overview of the HF and LF Noise Performances

S.D. Nsele, J.G. Tartarin, L. Escotte
LAAS-CNRS and University of Toulouse (UPS)
F-31031, Toulouse, France
tartarin@laas.fr

S. Piotrowicz, S. Delage
III-V Laboratory
91460, Marcoussis, France

Abstract— **From the first developments of Nitride technologies using AlGaN/GaN heterostructures for designing high power, high frequency HEMT devices, we now assist to the emergence of new declination with InAlN/GaN heterostructures. Considering the expected better interface quality of this last technology as a consequence of the better lattice match, and better electrical properties, these HEMT devices attract much interest for high frequency applications (transmitter for power, receiver for low noise and robustness versus jamming). Different InAlN/GaN technological developments have been studied considering their frequency and noise parameters for low noise amplifiers in Ka-band. The paper addresses two issues related to noise in InAlN/GaN HEMT devices; one concerns the study of the HF noise performance for different technological processes and for the optimized technology, whereas the second focuses on the gate and drain current LFN spectra of competing technological versions featuring good HF dynamic and noise performance.**

Keywords—Low Frequency Noise, High Frequency Noise, X and K band, InAlN/GaN HEMT

I. INTRODUCTION

Nitride technologies have registered a rapid growth during the last decade, especially on high power and high frequency segment markets. However, they are still far from exploiting their full potential. If AlGaN/GaN technologies are ready for market, they are regularly improving their reliability figures of merit (pushing the junction temperature and the mean time to failure for high power applications). One of the reasons why AlGaN/GaN devices need strong efforts concerns the electro-thermo-mechanical interactions that generate defects hampering to reach the ultimate potential of these technologies. An alternative has been found by using InAlN/GaN heterostructure featuring almost 18% of indium, which content is relevant with lattice match of the two materials. Moreover, the higher mobility and sheet density in the 2DEG is convenient for high power and high frequency applications. This work is part of the Genghis Khan project from the French National Agency for Research; the objective is to develop this technology for HF applications, through the design of a Ka-band transceivers. Part of the project, besides the technological issues, concerns the declination of an optimized low noise process for robust HF receivers: this paper addresses two

aspects of the noise studies through the analysis of HF and LF noise parameters. The first section presents the studies dedicated to high frequency noise on different technological processes, to find out the optimum declinations of the technologies for high frequency low noise applications. The second paragraph proposes investigations on low frequency noise for the selected technologies to detect some potential weaknesses of the transistor (traps), and to identify its technological maturity (1/f noise level).

II. HIGH FREQUENCY NOISE PARAMETERS

HF noise parameters are measured using different sub-bands for an overall possible frequency range from 4 GHz to 40 GHz. Devices under test have been characterized on 8 different processes featuring different gate length, gate width and gate-source gate-drain spacing, indium content between 18 and 21%, with different doping concentrations and passivation types. Electrical small signal models have been developed, and frequency dispersion effects have been evidenced over a large frequency range, up to few GHz; these rapid traps (or short term memory effects) impacting the GHz domain can strongly limit the performances of the devices for HF applications [1]. Medium and long term memory effects will also be evidenced in the section dedicated to LFN measurements. These trapping-detrapping HF mechanisms can also be illustrated in figure 1, where the minimum noise figure of merit F_{min} increases for decreasing frequencies below 8 GHz.
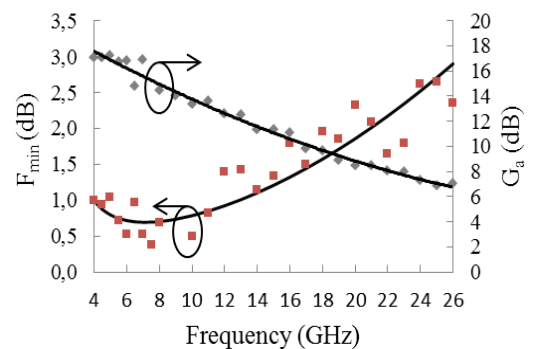

Fig. 1. Minimum noise figure F_{min} and Associated Gain G_a versus frequency for an InAlN/GaN MOS-HEMT (0.15x2x75µm², V_{DS}=5V and V_{GS}=-1V).

This behavior has been observed by Danneville et al. on GaAs FETs [2], and was attributed to shot noise. Fast traps affecting the transconductance and output conductance signatures versus frequency (as revealed for our devices), here combined with shot noise could explain this trend on F_{min}. The device under test from figure 1 features a transition frequency F_t=40 GHz and a maximum oscillation frequency F_{max}=70 GHz. The value of F_{min}=1.8 dB at 20 GHz (with associated gain G_a=8.8 dB) is still above that of AlGaN/GaN HEMT [3][4] or InAn/AlN/GaN transistors [5], featuring noise figures close to 1 dB at 26 GHz [5] or at 36 GHz [4] due to their low $L_G \le 0.1\mu m$. The reduction of the drain current largely affects the performances of F_{min}, as observed between HEMT and MOS-HEMT devices in figure 2. A reduction on F_{min} from 3.1 dB (HEMT) to 1.2 dB (MOS-HEMT) is obtained for 0.7 µm gate length devices, at 4 GHz.
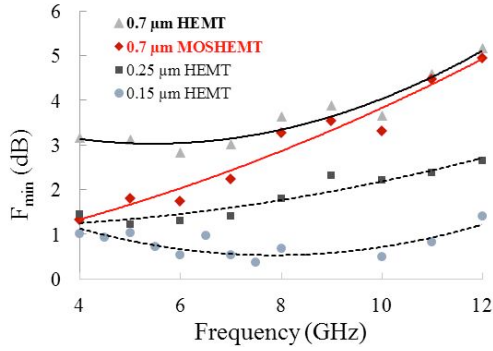

Fig. 2. Minimum noise figure F_{min} versus frequency for different InAlN/GaN HEMT and MOS-HEMT devices (measurements are given between 4-12 GHz).

However, MOS-HEMT devices feature slightly lower F_t and F_{max}, if compared with another competing technology with carbon doping (HEMT device featuring F_t=55 GHz and F_{max}=135 GHz): these two technologies can be used to design a 30 GHz LNA. Devices featuring 0.15µm or 0.25µm gate length have been studied for X-band and K-band applications. The optimum biasing point versus V_{GS} (or I_{DSS}/I_{DS}) and V_{DS} is mainly attributed to the elevated transconductance gain g_m condition, to the reduction of diffusion noise at low I_{DS} and to the management of self-heating effects under high dissipated power. An illustration of this optimum bias versus V_{DS} is given in figure 3.
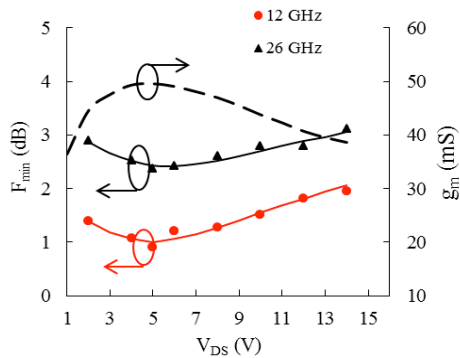

Fig. 3. Minimum noise figure F_{min} versus drain voltage V_{DS} for frequencies of 12GHz and 26GHz. Right axis represents the transconductance gain g_m.

F_{50} and four noise parameters measurements have been investigated and compared for X-band and Ka-band receiver's applications. F_{50} measurements are convenient for fast and systematic measurements as a first order analysis for biasing and sizing the device on each process declination, and also for a cross analysis between processes (with or without carbon doping, passivation type, indium content, gate length…). Then accurate characterization using the 4 noise parameters is performed (F_{min}, equivalent noise resistance R_n and complex optimum coefficient Γ_{opt}). Figure 3 presents the evolution of F_{50} versus $1/L_G$ at 18 GHz, for devices from the 8 different wafers under test: devices are biased at the minimum noise conditions. The influence of the dynamic performances (through the reduction of L_G) is noticeable on noise improvement.
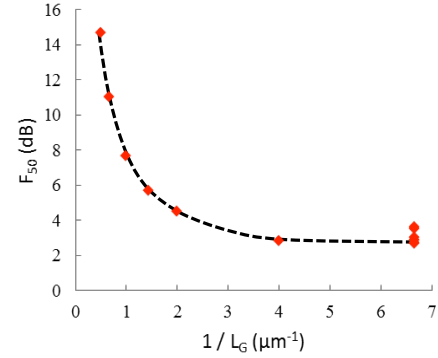

Fig. 4. F_{50} noise factor versus $1/L_G$: devices are biased at their optimum noise conditions (@18 GHz).

Figure 5 reports on the four noise parameters for a 0.15µm gate length device (plotted between 8-40 GHz). This device corresponds to the process and to the bias and size that will be implemented for the design of the robust LNA at 30 GHz, and presents a minimum noise figure of F_{min}=2 dB at 30 GHz.
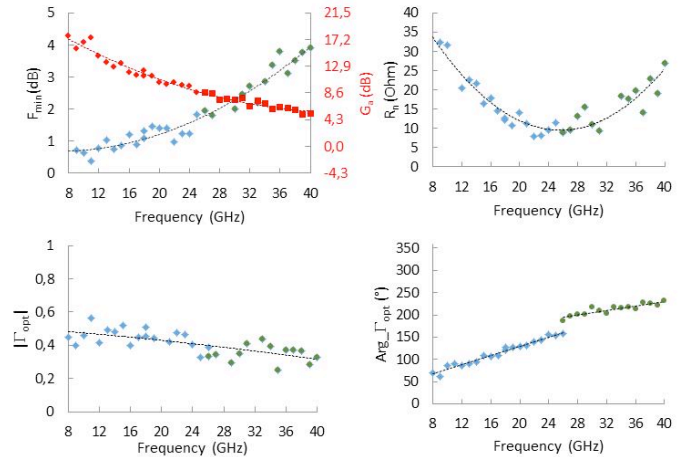

Fig. 5. Noise parameters F_{min}, R_n and Γ_{opt} (magnitude and argument) and associated gain G_a versus frequency (8-40 GHz) for the selected device (MOS-HEMT device feat. 21% In content, L_G=0.15µm, 2x75µm gate width, V_{DS}=6V and I_{DS}=20mA).

III. LOW FREQUENCY NOISE

In this paper, Low Frequency Noise (LFN) is used as a diagnostic tool to assess the quality of the processed MOS-HEMT evidencing the best HF performances from the previous study, and also on HEMT devices where Carbon has been used for doping. Gate and drain LFN current spectral density analysis of a transistor featuring 0.15μm of gate length are discussed. Measurements are performed between 1 Hz and 100 kHz, in two sub-bands for a better low frequency resolution. The two different processes that have been characterized feature almost the same characteristics in spite of differences (with or without carbon doping, passivation technique). The S_{IG} spectra presents different generation-recombination centers (GR) superimposed with the 1/f flicker noise. Moreover, some Lorentzian contributions can be attributed to random telegraph signal (RTS) measured in time domain on these transistors [6]. A distributed model is used to account for the 1/f like behavior, based on the plot of $S_{IG} \times$frequency versus frequency for an equally weighted extraction of the noise parameters. The contribution of the GR centers and of the distributed 1/f models are presented in figure 6, as well as the total fit and measurement of S_{IG}.
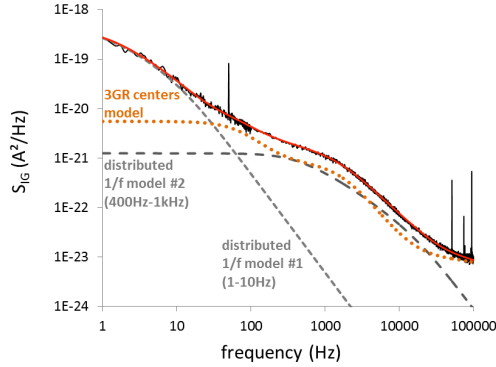

Fig. 6. Gate current spectral density S_{IG} versus frequency (open drain, V_{GS}=-1V), and associated model based on 2 distributed 1/f models (1-10Hz and 400-1000Hz) [6] and 3 GR centers (80Hz, 1.7kHz, and above 200kHz).

The evolution of the LFN spectra and of the fitting models is plotted in figure 7, for variable reverse V_{GS} biasing (identified by V_R).
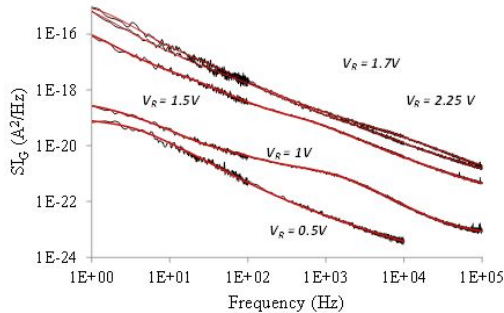

Fig. 7. Gate current spectral density S_{IG} versus frequency (open drain), for variable reverse gate bias V_R.

Time constants attributed to GR centers are extracted between 1 μs and 150 ms. One GR center depends on the static bias voltage V_{GS} (thermal conditions are stable when the drain is open); the logarithmic representation of its associated time constant evolves with the root square value of the electrical field according to Poole-Frenkel effect (the electrical field is extracted from a model using C-V measurements). Moreover, figure 8 plots the evolution of $S_{IG} \times$frequency versus I_{GS} for three different frequencies. This plot features a linear model $S_{IG} \approx I_{GS}^{\alpha}$, with α=3.3 or α=1.5 respectively for low and high levels of I_{GS}, and for different frequencies (10 Hz, 1 kHz, 100 kHz). This normalized representation establishes quite the same behavior versus I_{GS}.
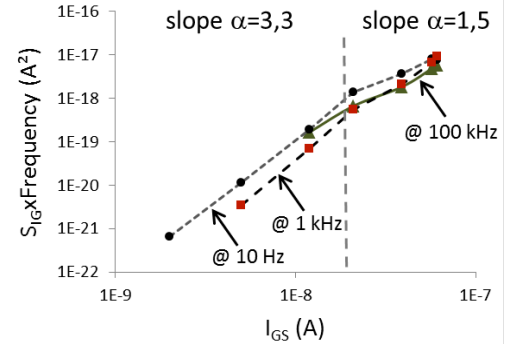

Fig. 8. $S_{IG} \times$frequency versus I_{GS} (at 1 Hz, 1 kHz, 100 kHz).

The different α values are attributed to different leakage mechanisms at low and high reverse V_{GS}. Electrical modelling of $I_{GS}(V_{GS})$ has evidenced different contributions to the reverse leakage current, with essentially Poole-Frenkel contribution before V_R=1V (i.e. I_{GS} below 30nA, as delimited in figure 8), and Fowler-Nordheim for higher reverse values of V_R (so for gate currents I_{GS}>30nA). This weight of each Poole-Frenkel or Fowler-Nordheim effect is correlated to the change in the slope on figure 8. The α=1.5 value is close to already published results on AlGaN/GaN HEMT [7]. As S_{IG} spectra evidence numerous GR centers, the slope of α=3.3 can be the consequence of these trapping-detrapping processes as stated previously by the time constant dependence with the root square of the electrical field for currents below 30nA (Poole-Frenkel contribution): indeed these GR centers are more pronounced at low V_R in figure 7 (i.e. low I_{GS} in figure 8) and trap–assisted mechanisms can be associated with this α=3.3 value.

Noise spectral densities have also been measured on the drain access, when the gate is short circuited. Figure 9 presents the variation of the normalized spectra S_{ID}/I_D when the gate voltage changes from open channel to pinch-off conditions. Only HEMT devices with carbon doping are presented and discussed for the drain current LFN measurements; indeed, these devices feature a non-monotonic atypical behavior of S_{ID} plot versus I_{DS} as shown in figure 10.
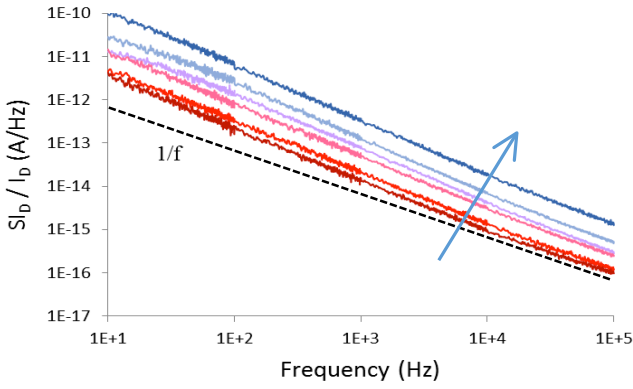
Fig. 9. Drain current spectral density S_{ID} versus frequency (gate short circuited), for variable V_{GS} (@V_{DS}=6V).

Generally, S_{ID} features an increase with I_{DS}, but for the device under test, a maximum is reached between pinch-off and open bias conditions in figure 10 (at V_{GS}=-1.5 V, i.e. I_{DS}=35mA). As a large number of GR centers have been found to be located at the InAlN/GaN interface, we suppose that the action of the gate bias on the conduction band can be the cause of this inflexion on S_{ID}. The maximum on S_{ID} also corresponds to the bias point where g_m is at its maximum, but even considering the carrier number fluctuation (and surface density of slow trap centers) the spectral density should not decrease. We formulate the next hypothesis for this decrease of S_{ID} when V_{GS} increases from V_{th} to 0V. The conduction energy band bends towards the GaN layer when V_{GS} increases; then the carriers are more distributed in the 2DEG volume, and less at the InAlN/GaN interface where traps are located. This is also convenient with the monotonic decrease of S_{ID}/I_D when the gate voltage V_{GS} shifts from V_{th} towards 0 V. When V_{GS} is near the pinch-off conditions, the conduction energy band confines the electrons close to this interface, and the normalized S_{ID}/I_D noise density is maximum.
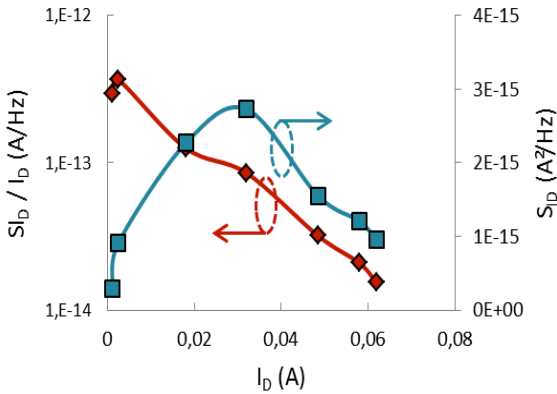

Fig. 10. Drain current spectral density S_{ID} and S_{ID}/I_D versus I_{DS} (@1 kHz, and for V_{DS}=6V).

Charges at the interface between InAlN/GaN are evidenced by S_{ID} and S_{ID}/I_D behaviors versus the biasing conditions of the device under test, as well as trapping effects on S_{IG}, with largely distributed effects [1].

IV. CONCLUSION

Wide bandgap InAlN/GaN MOS-HEMT and HEMT devices have been investigated in this paper: High frequency noise and Low Frequency Noise measurements have been performed on different technological processes. HF noise has been used to determine the optimum process for the design of a low noise amplifier in Ka-band: the effects of sizing, biasing and process variations (passivation types, doping levels) have been pointed out. F_{min}=1.9 dB have been measured at 30 GHz on MOS-HEMT devices. Low frequency noise performances have evidenced numerous GR centers on the gate current spectral density, some attributed to RTS noise. Moreover, the evolution of the drain current spectral density does present a maximum value versus I_{DS}, instead of a monotonic increase as expected, and as usually found in the literature. The bending of the conduction energy band with the gate-source voltage could explain a redistribution of the carriers more in the 2DEG, and less at the InAlN/GaN interface where traps have been localized. This is convenient with the behavior of the normalized S_{ID}/I_D which decreases with increasing I_{DS}.

REFERENCES

[1] S. Nsele, L. Escotte, J.G. Tartarin, S. Piotrowicz, S.Delage. "BroadBand Frequency Dispersion Modeling of the Output Conductance and Transconductance in AlInN/GaN HEMTs", IEEE Transactions on Electron Devices, April 2013, Vol. 60 , , pp.1372-1378

[2] F. Danneville, G. Dambrine, H. Happy, P. Tadyszak, A. Cappy, "Influence of the gate leakage current on the noise performance of MESFETs and MODFETs," Solid-State Electronics, vol. 38, no. 5, pp. 1081-1087, 1995.

[3] L. P. Smorchkova, M. Wojtowicz, R. Tsai, R. Sandhu, M. Barsky, C. Namba, P.H. Liu, R. Dia, M. Truong, D. Ko, J. Wang, H. Wang, and A. Khan, "AlGaN/GaN HEMT high-power and low-noise performance at f ≥ 20 GHz," in Proc. IEEE Lester Eastman Conf. on High Performance Devices, pp. 422-427, 2002.

[4] F. Medjoub, T. Tagro, M. Zegaoui, B. Grimbert, F. Danneville, D. Ducatteau, N. Rolland, P. A. Rolland, "Sub 1-dB minimum-noise-figure performance of GaN-on-Si transistors up to 40 GHz," IEEE Electron Device Letters, vol. 33, no. 9, pp. 1258-1260, 2012.

[5] P. Saunier, M. L. Schuette, T.-M. Chou, H.-Q. Tserng, A. Ketterson, E. Beam, M. Pilla, X. Gao, "InAlN barrier scaled devices for very high fT and low-voltage RF applications, " IEEE Trans. Electron Devices, vol. 60, no. 10, pp. 3099-3104, 2013.

[6] S. Nsele, L. Escotte, J.G. Tartarin, S. Piotrowicz, S.Delage. "Low-frequency noise in reverse-biased Schottky barriers on InAlN/AlN/GaN heterostructures", Applied Physics Letters, Vol.105, N°19, 192105p., Novembre 2014.

[7] J. G. Tartarin, S. Karboyan, D. Carisetti, B. Lambert, "Gate defects in AlGaN/GaN HEMTs revealed by low frequency noise measurement," International Conference on Noise and Fluctuations (ICNF) on IEEE, 2013.